Werk

Jahr: 1970
Kollektion: fid.geo
Signatur: 8 Z NAT 2148:36
Digitalisiert: Niedersächsische Staats- und Universitätsbibliothek Göttingen
Werk Id: PPN101433392X_0036
PURL: http://resolver.sub.uni-goettingen.de/purl?PPN101433392X_0036

LOG Id: LOG_0008
LOG Titel: Satellite techniques for observing water vapor-height profiles
LOG Typ: article

Übergeordnetes Werk

Werk Id: PPN101433392X
PURL: http://resolver.sub.uni-goettingen.de/purl?PPN101433392X

Contact

Niedersächsische Staats- und Universitätsbibliothek Göttingen
Georg-August-Universität Göttingen
Platz der Göttinger Sieben 1
37073 Göttingen
Germany
Email: gdz@sub.uni-goettingen.de

Zeitschrift für Geophysik, 1970, Band 36, Seite 1—25. Physica-Verlag, Würzburg

Satellite Techniques for Observing Water Vapor-Height Profiles[1])

By H.-J. Bolle, München[2])

Eingegangen am 11. März 1968

(In überarbeiteter Form am 18. Juni 1969)

Summary: Water vapor-height profiles can be derived from two different types of satellite measurements: firstly by analysing the spectrum of the outgoing thermal radiation, and secondly by measuring the absorption of solar radiation in the atmosphere.

The first method uses the remotely measured absolute intensities in the emission spectrum of the atmosphere. The vertical distribution of the emitting gas is inferred from these measurements with the aid of a mathematical inversion method. In a more direct approach this problem was first attacked by Möller for TIROS II data. Because of the limited spectral resolution it is only possible to determine the humidity of one broad atmospheric layer in the upper troposphere from measurements obtained with filter radiometers of the MRIR (medium resolution infrared radiometer) type. More sophisticated procedures have been developed since then in order to infer vertical constituent distributions from measurements of high spectral resolution.

The second method uses the occultation technique, and is limited to sunset and sunrise conditions. The main absorption in an optical path tangential to the earth occurs in a layer of about 6 km thickness near the minimum distance between this optical path and the ground. Spectral regions for this experiment must carefully be selected, and very high spectral resolution is necessary to detect small amounts of water vapor. However, this technique is promising to give water vapor concentration even in mesospheric levels which are inaccessible by the emission method.

Zusammenfassung: Wasserdampf-Höhenprofile können durch Messungen von Satelliten aus auf zwei verschiedene Weisen gewonnen werden: Erstens durch Analyse des Spektrums der den Planeten verlassenden thermischen Strahlung und zweitens durch Bestimmung der Absorption von Sonnenstrahlung beim Durchgang durch die Atmosphäre.

Die erste Methode verwendet die am Orte des Satelliten gemessenen absoluten Intensitäten im Emissionsspektrum der Atmosphäre. Daraus erhält man die vertikale Verteilung des emittierenden Gases mit Hilfe mathematischer Inversionsmethoden. Durch Anwendung eines direkteren Verfahrens hatte Möller diese Möglichkeit zuerst am Beispiel von Daten aufgezeigt, die mit dem Satelliten TIROS II gewonnen worden waren. Wegen der begrenzten

---

[1]) Vom Vorstand der DGG erbetener Übersichtsartikel.

[2]) Dr. Hans-Jürgen Bolle, Meteorologisches Institut d. Universität München, 8 München 13, Amalienstr. 52/III.

spektralen Auflösung läßt sich aus Messungen mit Infrarot-Radiometern mittlerer Auflösung (MRIR) nur die Feuchtigkeit in einer ausgedehnten Schicht der oberen Troposphäre bestimmen. Inzwischen sind jedoch verfeinerte Methoden ausgearbeitet worden, die es auch erlauben, die vertikale Verteilung atmosphärischer Gase aus Messungen mit hoher spektraler Auflösung abzuleiten.

Die zweite Methode benutzt die Okkultationstechnik und ist dadurch nur bei Sonnenaufgang und Sonnenuntergang anwendbar. In einem tangential zur Erde verlaufenden optischen Weg wird der überwiegende Teil der Sonnenstrahlung in einer etwa 6 km hohen Schicht nahe dem Minimalabstand vom Boden absorbiert. Die in einem solchen Experiment zu verwendenden Spektralbereiche müssen sorgfältig ausgewählt werden und eine hohe spektrale Auflösung ist notwendig, um noch kleine Wasserdampfmengen nachweisen zu können. Mit Hilfe dieser Technik sollte jedoch der Wasserdampfgehalt bis in die Mesosphäre hinein meßbar sein.

1. Introduction

The continuous sensing of the water vapor concentration in the atmosphere and its variations in space as well as in time is one of the principal tasks of meteorology in the age of satellite exploration. The reasons for this desire are easily recalled.

Water vapor is the most variable of all minor constituents of the atmosphere and is thus involved in many of the meteorological processes (see Table 1):

1. The water vapor is regulating the heat budget of the lower atmosphere by absorbing and emitting infrared radiation, and by condensation as well as evaporation processes. The inclusion of these effects in the mathematical model of the atmosphere promises improvements of numerical forcast capabilities.
2. Changes of tropospheric and lower stratospheric moisture are indicators for air mass boundaries, and for vertical convection.
3. The humidity of the stratosphere and mesosphere affects the radiation balance of these levels, and plays a rôle in the photochemistry of the upper atmosphere.

The humidity of the lower atmosphere up to the tropopause is relatively well known by routine soundings. However, there exist large gaps over the oceans. Much more difficult is the determination of stratospheric and mesospheric moisture by direct methods. In the application of hygrometers, mass spectrometers, and spectroscopic methods from balloons or rockets always contamination, radiation errors as well as effects of the individual instruments have carefully to be considered, and only sporadic measurements from a small number of fixed sites are possible. Satellite observations have the great advantage to give global observations with one and the same instrument, and much more geographical fine structure, when the problem of remote sensing is solved satisfactorily.

Satellite observations of water vapor are only possible by radiometric measurements in the infrared or in the microwave region. Performance and interpretation of such measurements require a detailed quantity of knowledge about water vapor and its infrared spectrum. The activity in this field was to a good deal pushed forward by GATES who made the first attempt to measure the spectrum of the stratosphere from a balloon [GATES, MURCRAY, SHAW and HERBOLD 1958].

Table 1: Atmospheric phenomena linked to water vapor distribution.

REGION	PROCESSES AFFECTED BY WATER VAPOR	PROCESSES AFFECTING WATER VAPOR DISTRIBUTION	CLOUDS
MESOSPHERE	HEAT BUDGED UV AND IR ABSORPTION IR EMISSION OH-EMISSION THROUGH $O(^1D)+H_2O \longrightarrow 2OH$ O_3 - CONCENTRATION (?)	DIFFUSION PHOTOCHEMICAL REACTIONS GENERAL CIRCULATION AND WAVE MOTIONS	NOCTILUCENT
STRATOSPHERE	THERMODYNAMIC EQUILIBRIUM ABSORPTION AND EMISSION OF IR RADIATION	LARGE SCALE MIXING, TRANSPORT	NACREOUS
TROPOSPHERE	THERMODYNAMIC EQUILIBRIUM ABSORPTION AND EMISSION OF IR RADIATION	CONDENSATION EVAPORATION PRECIPITATION CONVECTION ADVECTION	ICE AND WATER

This experimental work was continued by MURCRAY [MURCRAY, WILLIAMS, and LESLIE 1960], and was supported by extensive laboratory studies of the water vapor absorption spectrum [HOWARD, BURCH, and WILLIAMS 1956; PALMER 1957, 1960; BURCH, GRYVNAK, SINGLETON, FRANCE, and WILLIAMS 1962; BURCH, GRYVNAK and PATTY 1965; BURCH and GRYVNAK 1966; SAKAI 1964; OPPENHEIM and GOLDMAN 1966; PRINZ 1968]. At the same time most essential progress was made in the theoretical understanding of the spectrum [ANDERSON 1949; YAMAMOTO and ONISHI 1949, 1951; HERZBERG 1962; TSAO and CURNUTTE 1962; BENEDICT and KAPLAN 1959, 1964; GATES, CALFEE, HAUSER, and BENEDICT 1964; BENEDICT and CALFEE 1967], and in the theory of radiative transfer [CURTIS and GOODY 1956, GOODY 1964].

In this survey we will discuss the state of the art of two different experimental approaches: The first utilizing the emission, the second the transmission technique.

2. Emission Measurements

If a spectral radiometer looks down from a satellite into the atmosphere within spectral intervals where water vapor absorbs and emits infrared radiation, e.g. in the 6.3 micron band or the pure rotational spectrum beyond 16 micron, it will receive more or less radiation energy depending on whether the source—in our case the water vapor—is concentrated in warmer or colder levels of the atmosphere. Let us first consider a detector which is sensitive in a broad spectral band. In this case only the emission of the troposphere is of importance. A dry atmosphere is then associated with strong emission because lower and warmer levels of the atmosphere near the ground contribute strongly. A large amount of humidity in higher and colder levels create small radiation signals, because the emission of the lower levels is screened by these higher layers. With the MRIR (Medium Resolution Infrared Radiometer) there are observed patterns like those shown in Figures 1 and 2 from NIMBUS III. The picture of the 6.5—7.0 micron channel (the center of one of the ν_2 H_2O branches) differs in some details from the simultaneous measurement in the 10—11 micron region which shows the bright cloud structure against the strong emitting dark ground. Though most of the structure to be seen in the 6.7 micron channel is due to high clouds (> 6 km), some of the brighter spots lead to the conclusion that the clouds are accompanied by clusters of water vapor at higher levels, and that the dark areas between these spots show dry spaces of subsiding air. This was especially obvious during orbit 391 of NIMBUS II. Here the hurricane Alma (1966) was already in the decaying stage with lower and warmer clouds (to be recognized in the 10—11 micron channel) but still high humidity at higher levels indicated by the bright picture in the water vapor channel. The spiral of the vortex was clearly to be seen with a dry band wound up several times in the storm [NORDBERG, MCCULLOCH, FOSHEE and BANDEEN 1966]. A similar example is given in Fig. 2. The gray scale of the pictures can directly be calibrated into equivalent black body temperatures and from these temperatures the height of the emitting water vapor layer can be deduced if the temperature profile of the atmosphere is known.

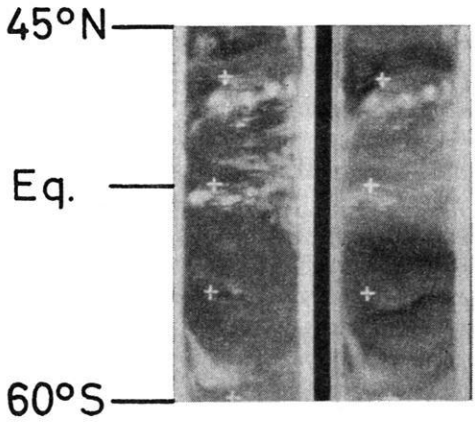

Fig. 1. Section of MRIR-picture from NIMBUS III, 7. 7. 1969, 18.10.—18.42 GMT (local night). Left part 10—11 μ channel, right part 6.5—7 μ channel. The strip ranges from approximately 60°E to 90°E at the equator. It shows an area with broken clouds and mostly high water vapor concentration at elevated levels (bright areas in the right picture) but marked subsidence zones (dark bands) of dry air in between. Courtesy A. W. McCulloch, GSFC.

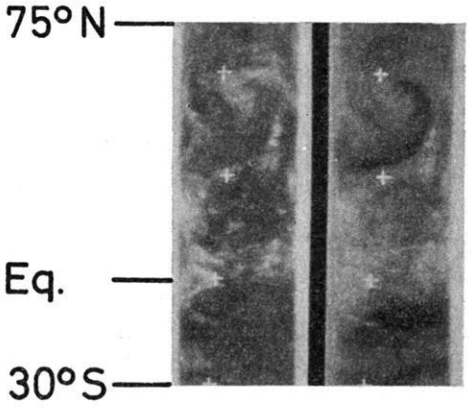

Fig. 2. Section of MRIR-picture from NIMBUS III, 18. 7. 1969, 16.05—16.37 GMT (local night). Left part 10—11 μ channel, right part 6.5—7 μ channel. The strip ranges from approximately 90°E to 120°E at the equator. A decaying vortex with humid air at elevated levels can clearly be distinguished between 30°N and 60°N. A band of dry air is wound up into the cyclone. Another area of subsiding air can be distinguished at 10°S, 95°E to 115° south of Sumatra and Java. Courtesy A. W. McCulloch, GSFC.

Let us now assume a cloud-free atmosphere with an uniform relative humidity and a known lapse rate. For this case Möller [1961] could show, by computing various models, that the equivalent emission temperature in the 6.5 micron channel is mainly

a function of relative humidity and surface temperature, but depends only slightly on the actual atmospheric temperatures. Based on this simple model MÖLLER [1962] worked out a method to infer the relative humidity from measured radiances. The principle of this method is demonstrated in Figure 3 where the emission function is plotted against height for 100% and 5% humidity. The area under these curves gives the emitted radiance, which is regarded as a function of the mean relative humidity in the 5—15 km layers only. No radiation of the earth's surface penetrates through the atmosphere in the considered spectral region of the 6.3 micron water vapor band. This situation can be different if high clouds are present. One and the same measured radiance may then suit a dry atmosphere with a cold cloud top as well as a humid atmosphere with a warm cloud top. To make a decision between these possibilities a second independent measurement is necessary which MÖLLER found in the 8—12 micron channel that gives the nearly genuine surface temperature. The method has further been developed by RASCHKE [1965] for TIROS III observations. The work culminated in quasi-global representations of mean relative humidity in the upper troposphere,

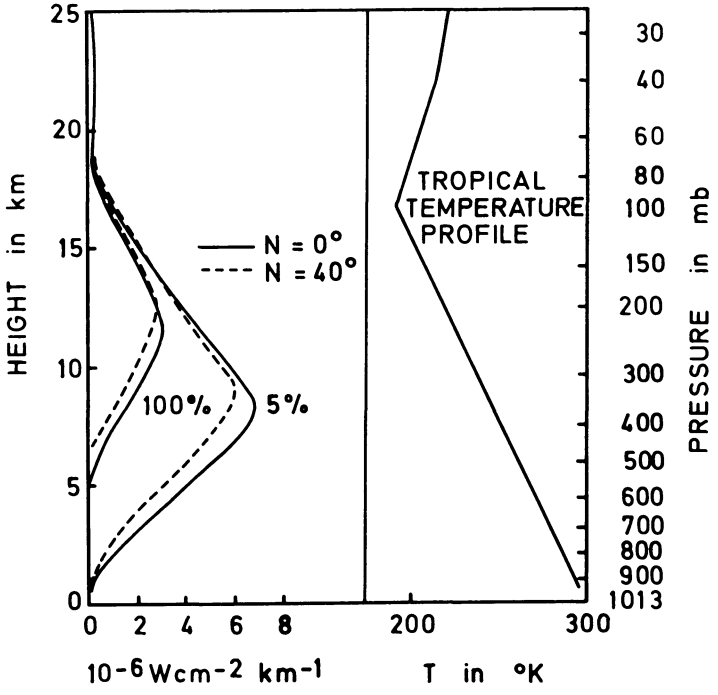

Fig. 3: Emission function for channel 1 (6.3±0.5 micron) of TIROS IV in a tropical model atmosphere with constant relative humidity (100% and 5%). After RASCHKE and BANDEEN [1966].

and the determination of the water vapor mass above 500 mb for six months from TIROS IV measurements by RASCHKE and BANDEEN [1966]. Figures 4 and 5 show examples of this serie.

On principle it is not possible to derive from measurements in one spectral channel only a more detailed picture of the vertical water vapor distribution than one mean value for the upper troposphere. Spectral measurements with high resolution as firstly proposed by HANEL [1965] and presently obtained from NIMBUS III give a much more detailed picture of the water vapor emission spectrum, and offer therefore the possibility to apply more sophisticated mathematical inversion methods to water vapor distribution. The problem has recently been formulated by CONRATH [1966, 1967, 1968]. The spectral radiance N_ν reaching the satellite is given by

$$N_\nu = \int_{h\infty}^{h_0} \frac{\partial B_\nu[T(h)]}{\partial h} \tau_\nu[m(h, h_\infty)]\, dh \tag{1}$$

where B is the PLANCK function, T the temperature, τ the transmission function, ν the wavenumber, h the height, and $m(h, h_\infty)$ the water vapor mass between the height h and the top of the atmosphere, which has to be inferred. Ground contribution has been neglected in equation (1) for simplicity. With $m(h, h_\infty) = u(x)$ it follows

$$\tau_\nu[m(h, h_\infty)] = \tau_\nu[u(x)] = \tau_\nu[u_0(x)] + \left(\frac{\partial \tau}{\partial u}\right)_{u_0(x)} \delta u(x) \tag{2}$$

where $u_0(x)$ is a "first guess" at the solution. With x_s being the value of x at the surface, equation (1) can be written:

$$N_\nu = \int_0^{x_s} \frac{\partial B_\nu(x)}{\partial x} \tau_\nu[u_0(x)]\, dx + \int_0^{x_s} \frac{\partial B_\nu(x)}{\partial x} \left(\frac{\partial \tau_\nu}{\partial u}\right)_{u_0(x)} \delta u(x)\, dx\,. \tag{3}$$

x is the pressure P, $\log P$ or another single valued function of P. The problem reduces to the solution of

$$g_{0,\nu} = \int_0^{x_s} K_{0,\nu}(x)\, \delta u(x)\, dx \tag{4}$$

if the following abbreviations are used:

$$g_{0,\nu} = N_\nu - \int_0^{x_s} \frac{\partial B_\nu(x)}{\partial x} \tau_\nu[u_0(x)]\, dx \tag{5}$$

$$K_{0,\nu} = \frac{\partial B_\nu(x)}{\partial h} \left(\frac{\partial \tau_\nu}{\partial u}\right)_{u_0(x)} \tag{6}$$

From the first approximation $u_0(x)$ an initial weighting function can be derived. By an iterative process of setting

$$u_n(x) = u_{n-1}(x) + \delta_n u(x) \tag{7}$$

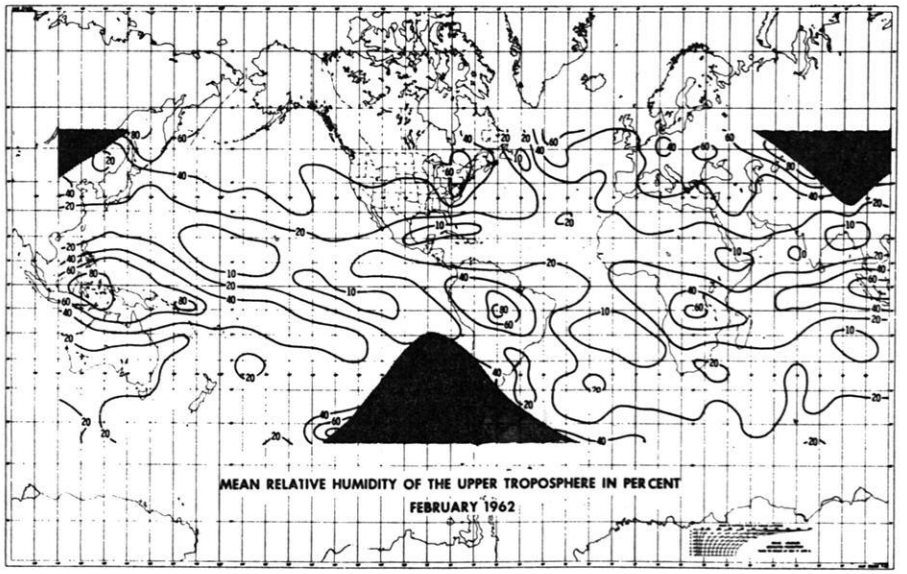

Fig. 4: Mean relative humidity of the upper troposphere in percent from TIROS IV measurements. February 1962. After RASCHKE and BANDEEN [1966].

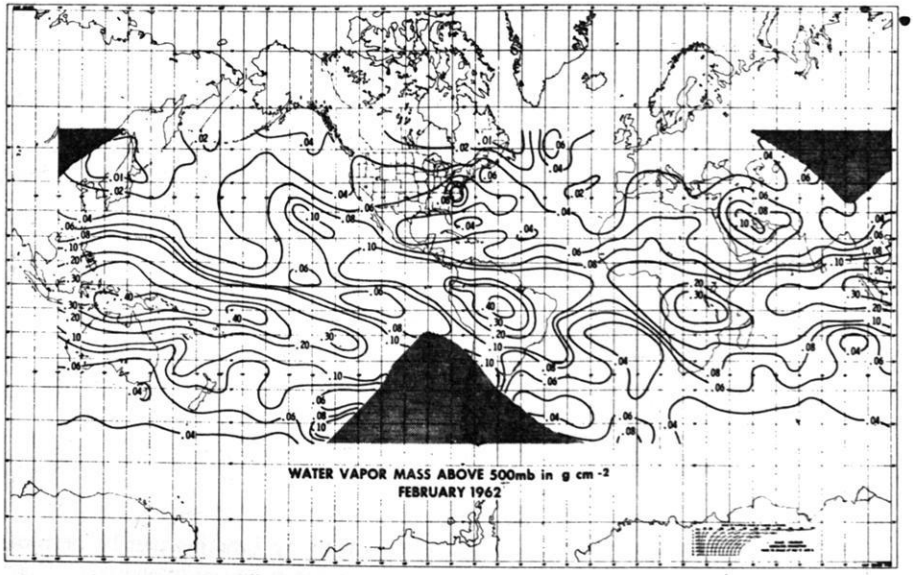

Fig. 5: Mean water vapor mass above 500 mb in g cm^{-2} from TIROS IV measurements. February 1962. After RASCHKE and BANDEEN [1966].

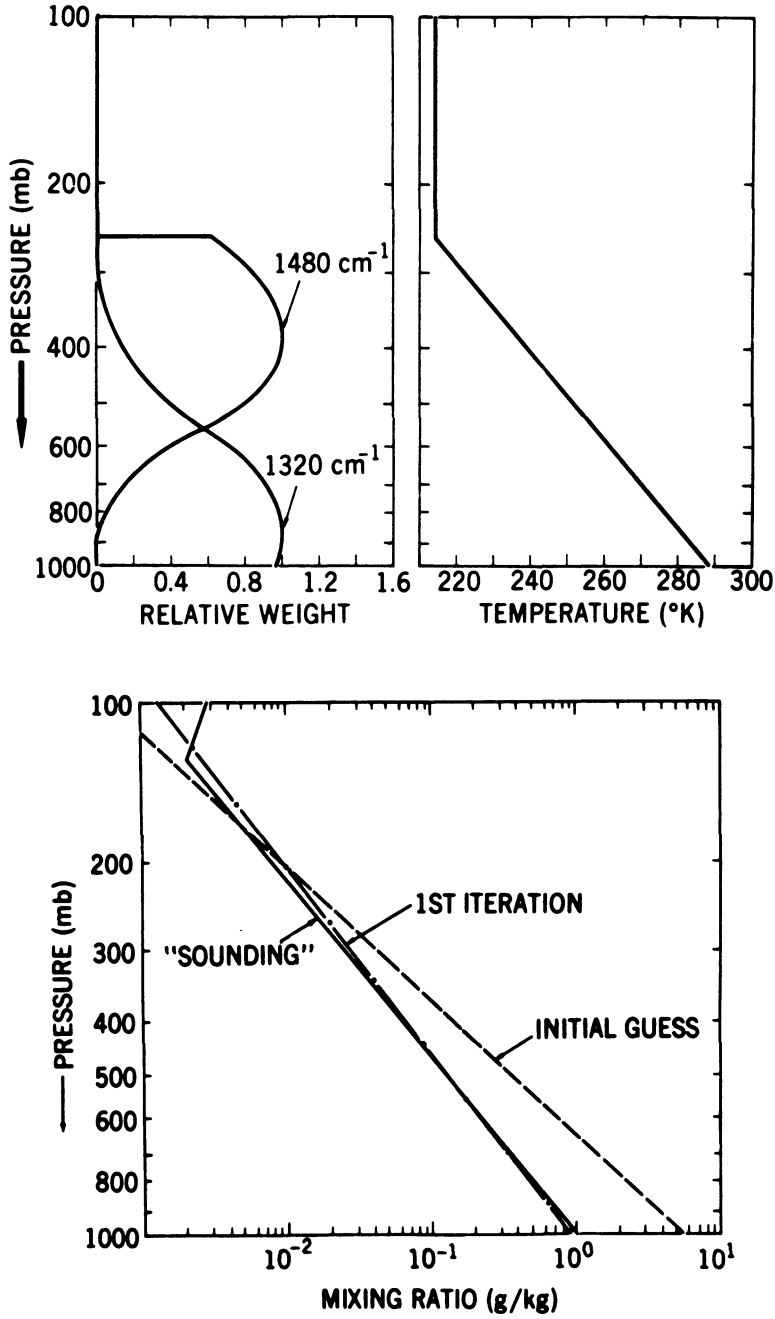

Fig. 6: Weighting functions and temperature profile employed by CONRATH [1967] in the water vapor inversion (upper part). The resulting inversion of synthetic date is shown in the lower figure.

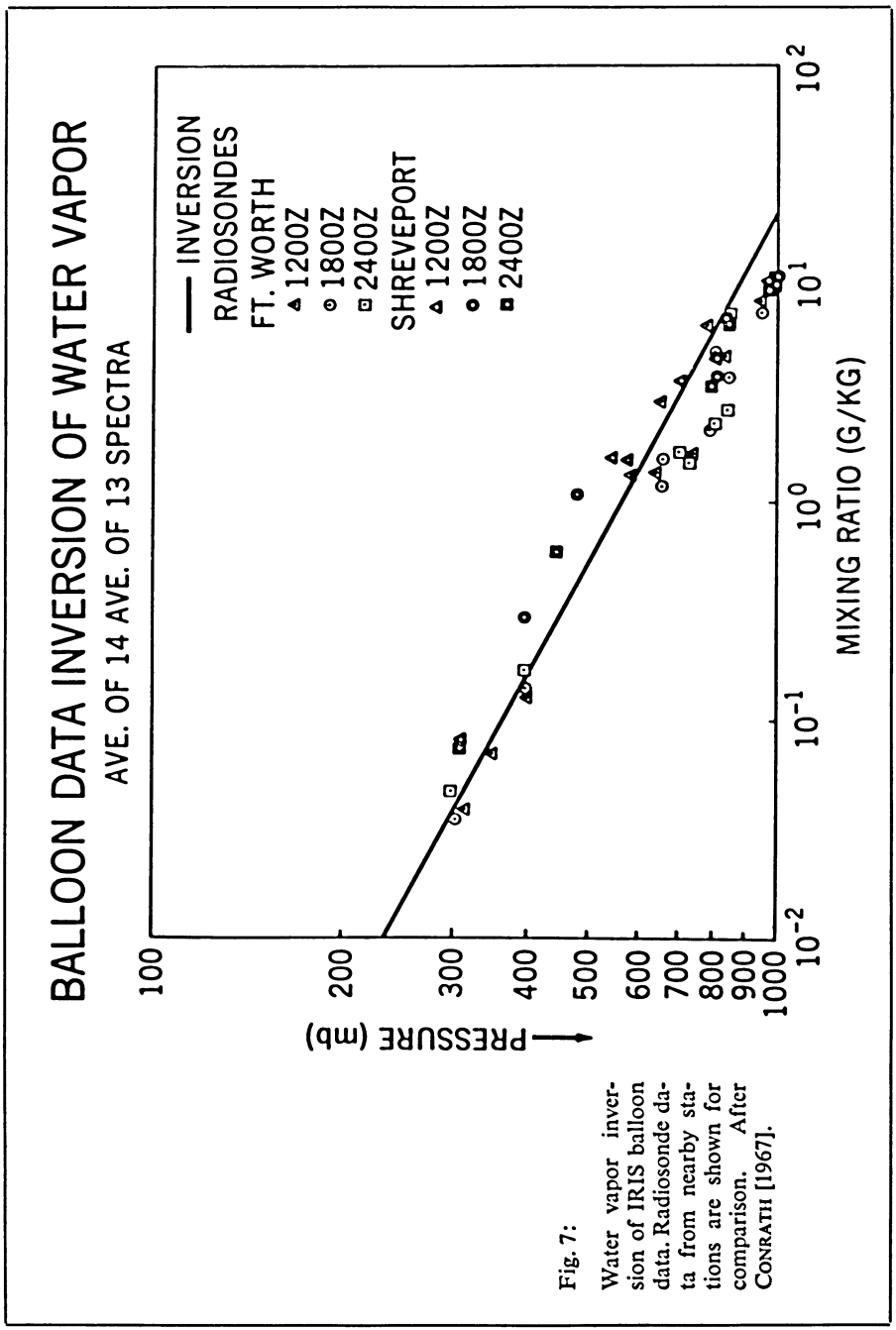

Fig. 7:
Water vapor inversion of IRIS balloon data. Radiosonde data from nearby stations are shown for comparison. After CONRATH [1967].

equation (4) can in principle be solved for as many parameters (e.g. mixing ratio in different levels or gradients) as measurements in spectral regions with different weighting functions are available. However, the precision of the measurements sets severe limits to the number of available informations. The solution becomes more and more instable with increasing numbers of inferred parameters if the experimental error is not infinitly small.

Figure 7 shows the water vapor mixing ratio which was inferred from balloon-borne interferometer-spectrometer measurements, using a very simple two-parameter model (Fig. 6) of the water vapor distribution:

$$q(P)=q_s\left(\frac{P}{P_s}\right)^r, \tag{8}$$

where $q(P)$ is the mixing ratio at pressure P, q_s the mixing ratio at surface pressure P_s, and r the pressure exponent of the mixing ratio. This notation is equivalent to

$$u(x)=u(P)=u_s\exp\left[-2.303\,(r+n+1)\log(P/P_s)\right] \tag{9}$$

with $u_s = q_s P_s/g\,(r+n+1)$. n is the pressure exponent for the reduced absorber mass, this reduction being necessary because of the dependency of linewidth on pressure. q_s and r are the parameters to be determined.

There are different other mathematical constituent inversion methods proposed (see e. g. KING [1963], SMITH [1967, 1968], KUHN and MCFADDEN [1967]), but the discussion of these methods lies beyond the scope of this review. It shall be sufficient to state here that constituent inversion is possible, and has already been applied to the tropospheric water vapor. A difficulty exists for the isothermal region in the lower stratosphere, because here a change in humidity does not have much influence in the effective radiation temperature. Only the total amount of water vapor can be derived for isothermal layers, if channels with weighting functions below and above this layer are provided.

The stratospheric water vapor can only be considered if measurements are made in very narrow spectral intervals of high absorption as occur in the center of the pure rotation band. It is therefore highly recommended to extend spectral measurements to wavenumbers down to 200 cm^{-1} or less. These longer wavelengths may also be favoured because of the following reasons: (i) the influence of atmospheric dust decreases with increasing wavelength, and (ii) the longer wavelengths are less affected by the emission of other atmospheric constituents. The 6.3 micron water vapour band is superimposed by CH_4, N_2O, and O_3 bands, and an emission of still unknown origin (PICK and HOUGHTON [1968]). Figure 9 shows the emission spectrum to be expected from different model atmospheres as shown in Figure 8, around 202 cm^{-1} wavenumber with a magnification of the part around the very strong lines near 202.67 cm^{-1} in Figure 10. Figure 11 gives the weighting function for different bandwidths. The variation of the weighting functions in different atmospheres is demonstrated in Figure 12.

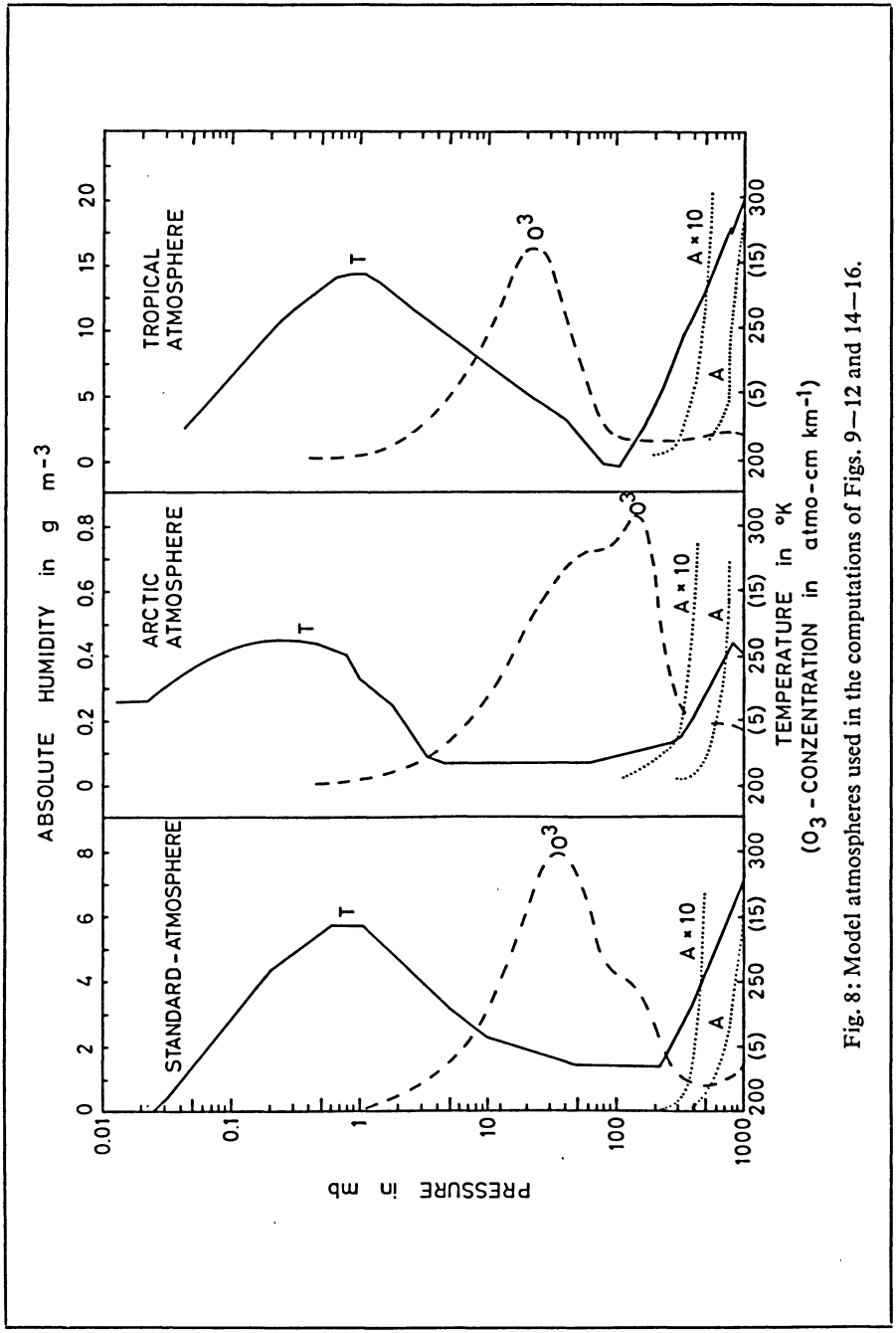

Fig. 8: Model atmospheres used in the computations of Figs. 9—12 and 14—16.

At higher levels than approximately 30 km, however, the emission is concentrated to such narrow intervals in the cores of the strongest lines that its measurement is hopeless with the techniques in practice. The selective filter method of HOUGHTON [1961] and SMITH [SMITH and PIDGEON 1964] seems to be very difficult to apply for water vapor because condensation and evaporation in the cell would probably cause severe trouble.

3. Transmission Measurements

In the stratosphere and perhaps also in the mesosphere another technique is promising for the future: the occultation experiment. The principle is demonstrated in Figure 13. In this experiment the sun is taken as source for a measurement of the atmospheric transmission in an optical path tangential to the earth. In the long optical paths obtained in this way a small water vapor concentration still gives a measurable absorption. The measurement, however, is restricted to sunrise and sunset. The method was first proposed for O_3 by FRITH [1962].

The inversion of the data is strongly facilitated if one can choose spectral regions where the temperature has a negligible effect on the transmission functions [BOLLE 1965]. Such regions occur for lines of distinct rotational transitions. One of the most prominent line groups which satisfies this condition consists of the three strongest

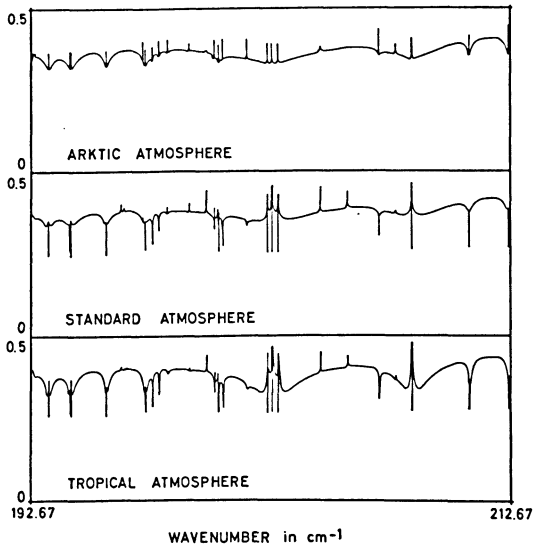

Fig. 9: Computed emission spectra of atmospheric water vapor in the 193—213 cm^{-1} region for the three model atmospheres of Fig. 8 in the sequence arctic, standard and tropical atmosphere. Water vapor mixing ratio is $10^{-5}\ g/g_{air}$ for standard and tropical atmosphere, and $2 \cdot 10^{-6}\ g/g_{air}$ for arctic atmosphere. Line data of BENEDICT and KAPLAN [1963] have been used.

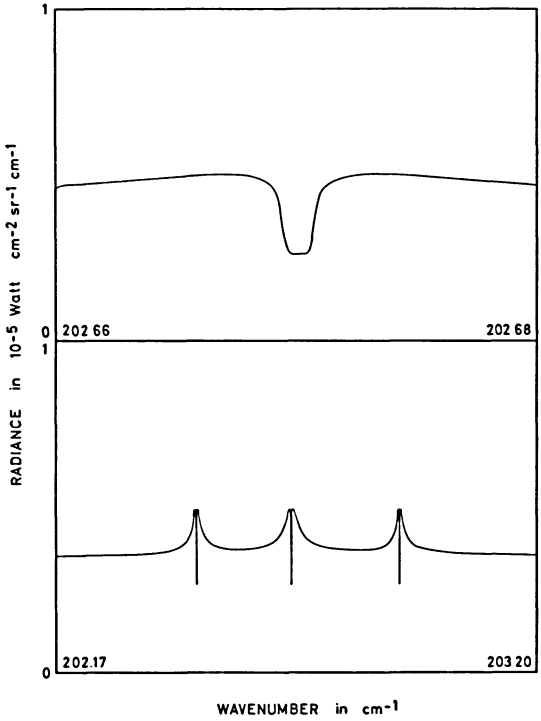

Fig. 10: Computed emission of atmospheric water vapor near 202.67 cm^{-1} from a standard atmosphere into space. Data from Fig. 9 in extended wavenumber scale.

water vapor lines between 202.46 and 202.97 cm^{-1}. The computed transmission of a model atmosphere in this spectral interval for different minimum heights of the optical path above ground (see Figure 13) is shown in Figure 14. The Figure also demonstrates the height resolution obtainable without application of mathematical inversion methods: the weighting functions are plotted at the right side of the transmission spectra. They are concentrated around the point of minimum height and their half widths reach from 0.5 to 6 km above this level. The equivalent widths of the strongest lines and line groups in the pure rotational band, the ν_2 and the ν_3 band, are given in Figures 15 and 16. From these figures it is obvious that the lines with the largest intensity do not always give highest absorption at high levels, because in the upper atmosphere not the LORENTZ-broadening but the DOPPLER-broadening is the dominant effect, and the DOPPLER-half width increases with the wavenumber. However, the transmission becomes nearly independent of absorbed mass in the transition region between collision and DOPPLER-broadening, and this transition occurs at lower levels for higher frequencies. This effect favours the longer wavelengths for measurements in the D-region.

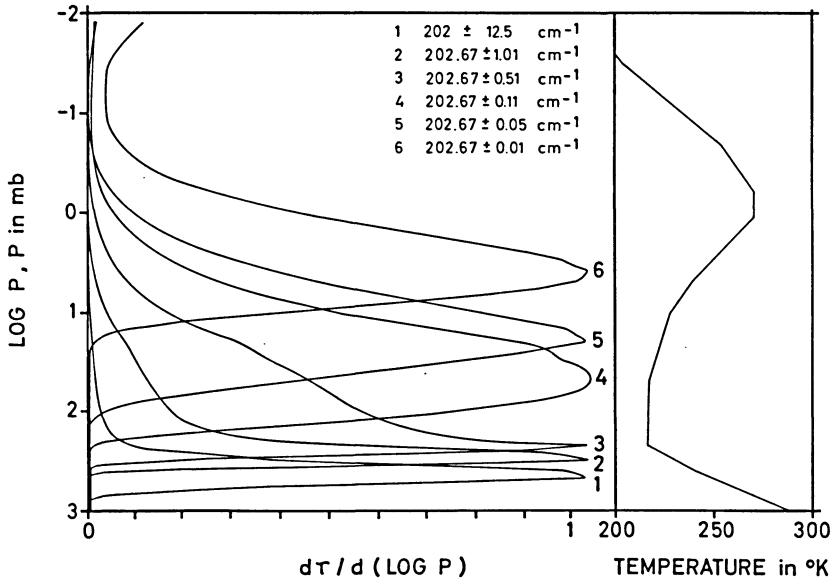

Fig. 11: Normalized weighting functions for emission of atmospheric water vapor in the 200 cm^{-1} region for different bandwidths. Standard atmosphere (see Fig. 8) with 10^{-5} g/g_{air} water vapor in the stratosphere.

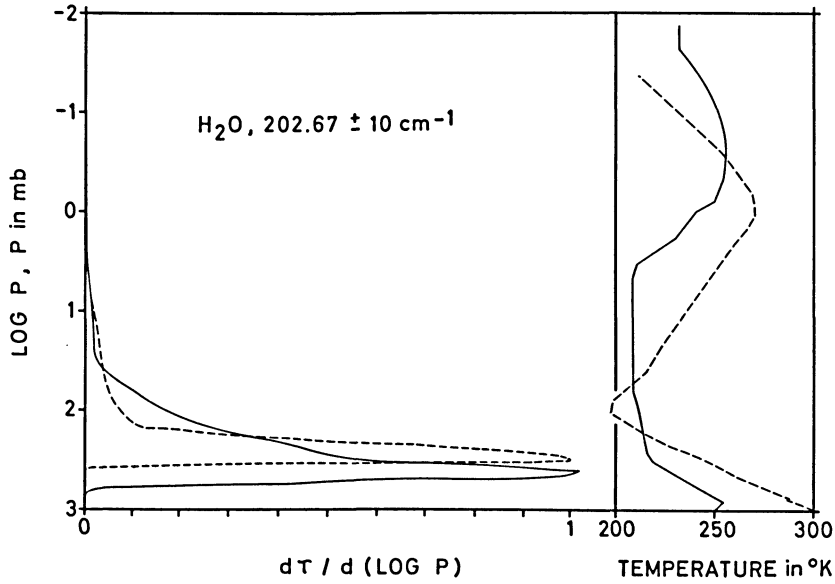

Fig. 12: Normalized weighting functions for emission of atmospheric water vapor in the 202.67 $\pm$ 10 cm^{-1} region in an arctic and a tropical atmosphere. Stratopheric mixing ratio $2 \cdot 10^{-6}$ g/g_{air} respectively 10^{-5} g/g_{air}.

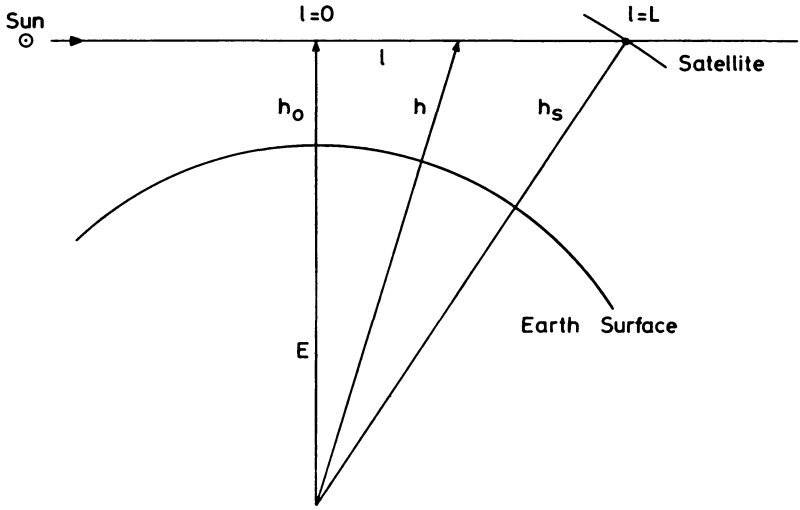

Fig. 13: Scheme of occultation experiment. H_0 is the minimum distance of the optical path from the earth surface.

The height limit for the application of the occultation technique is set by the spectral resolution as well as the available solar energy. The solar radiation is approximately that one of a black body of 6000 °K in the near and medium infrared but seems to drop to 4500 °K beyond 200 cm^{-1} [BEER 1966]. From this point of view near infrared wavelengths are superior to longer wavelengths, though the far infrared spectrum is less affected by other absorbers and scattering due to possibly existing aerosol layers. With the techniques in development it seems to be possible to measure equivalent line widths of 0.5 cm^{-1} to an accuracy of 1—2%, or to "detect" lines down to $\sim$ 0.01 cm^{-1} equivalent width. This will be enough to measure stratospheric water vapor to $\pm$ 10% if the mixing ratio lies between 10^{-6} g/g_{air} and 10^{-5} g/g_{air}. At 80 km the magnitude of water vapor concentration can still be determined if larger than 10^{-6} g/g_{air}. Table 2 summarizes some of the data on which this statement is based. A promising inversion method for this type of data has recently be developed [LATKA 1969], and its capability to invert simulated measurements has been demonstrated even with a strong inversion in the vertical water vapor distribution—like case 3 in Fig. 15. The instrument proposed for the measurements is a SISAM-type interferometer [CONNES 1959, 1960; VÖLKER 1969].

A problem exists in the proper alignment between the optical axis of a spectral radiometer and the solar pointing control necessary for this experiment. While the sun sensors are operating in absorption-free regions in the visible, the absorption measurement has to be done in very narrow spectral intervals of high absorption where large and rapid changes of the refractive index occur as demonstrated in Figure 17. This

Table 2: Requirements for the water vapor occultation experiment.

HEIGHT in km	PRESSURE in mb	H_2O - MASS IN OPTICAL PATH FOR MIXING RATIO 10^{-5} g/g$_{air}$	DETECTABLE H_2O - MASS			
			202 cm^{-1}		3838 cm^{-1}	
			FOR MEASURABLE EQUIVALENT WIDTH OF			
			0.01	0.1	0.01	0.1
			cm^{-1}			
16	100		$1.0 \cdot 10^{-7}$	$4.0 \cdot 10^{-6}$	$1.0 \cdot 10^{-6}$	$2.0 \cdot 10^{-5}$
31	10	$1 \cdot 10^{-4}$	$4.0 \cdot 10^{-7}$	$4.0 \cdot 10^{-5}$	$1.4 \cdot 10^{-6}$	$2.0 \cdot 10^{-4}$
49	1	$9 \cdot 10^{-6}$	$4.0 \cdot 10^{-6}$	$4.0 \cdot 10^{-4}$	$1.5 \cdot 10^{-6}$	$2.7 \cdot 10^{-3}$
66	0.1	$1 \cdot 10^{-6}$	$3.5 \cdot 10^{-5}$	$3.5 \cdot 10^{-3}$	$1.5 \cdot 10^{-6}$	$2.0 \cdot 10^{-2}$
80	0.01	$1 \cdot 10^{-7}$	$2.0 \cdot 10^{-4}$	$2.0 \cdot 10^{-2}$	$1.5 \cdot 10^{-6}$	0.15
SOLAR FLUX in watts cm^{-2} cm			10^{-8}		$3 \cdot 10^{-6}$	
NECESSARY AREA in cm^{-2} FOR COLLIMATOR OPTICS IF DETECTOR $D^* = 10^{-8}$ watts^{-1} HZ$^{1/2}$ AND PRECISION OF MEASUREMENT						
1%			10^4	10^3	30	3
10%			10^3	10^2	3	0.3

The missing number in the first line reads 0.06 g.

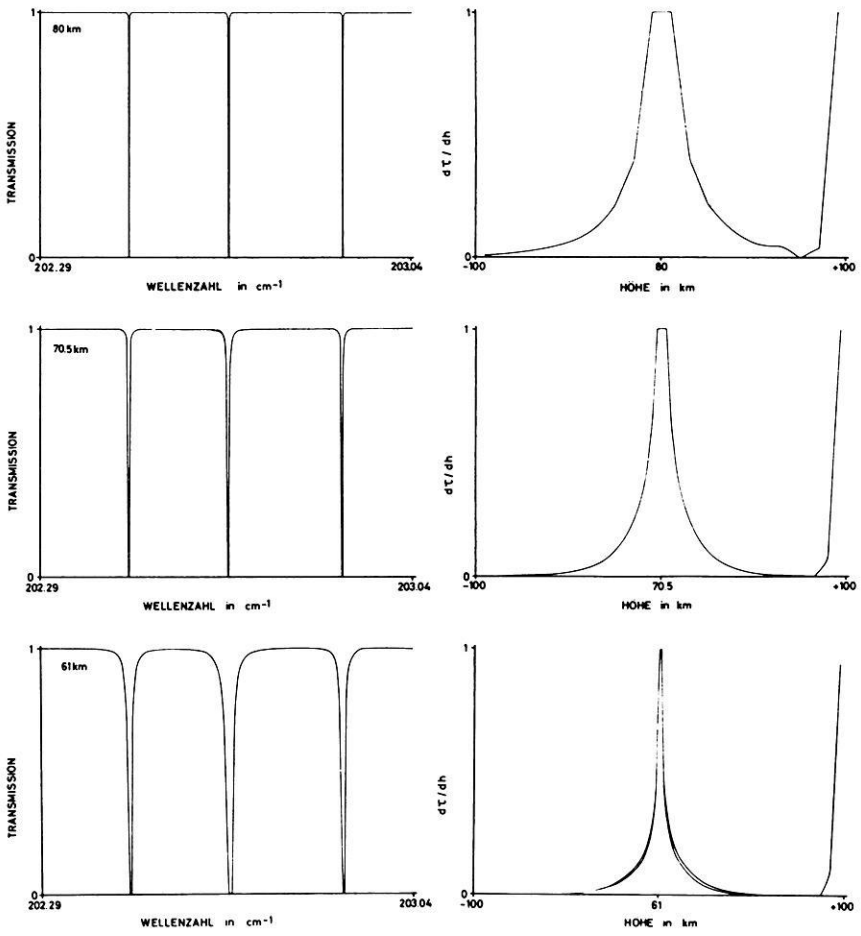

Fig. 14: Computed transmission spectra 202.29—203.04 cm^{-1} for occultation experiment conditions in dependence of minimum distance between optical path and earth surface. Water vapor mixing ratio $10^{-5} g/g_{air}$, Standard Atmosphere. At the right side of each spectrum are monochromatic weighting functions for different wavenumbers in the central line. The weighting function at the extreme right corresponds always to the line center. The solar radiation comes from the right side. The minimum heights of the calculations are (from the upper left to the lower right): 80, 70.5, 61, 50.5, 42.69 and 37.42 km.

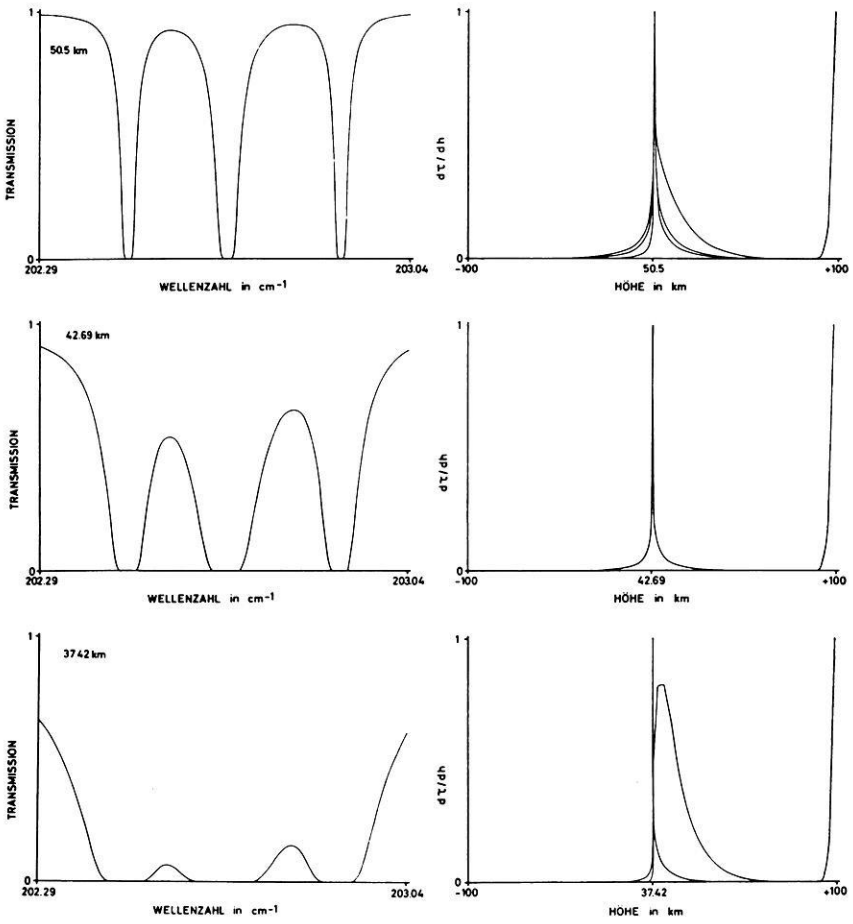

Zu Fig. 14.

effect leads to a deviation of the optical path near absorption lines which can affect the transmission measurement: the radiometer "looks" beside the sun around half-width distance from the line center. It can be neglected at higher levels. On the other hand proposals have been made to measure this refraction for lower lines of sight, and to use it as an independent method of water vapor determination.

4. Resumé and outlook

From high spectral resolution experiments presently flown on NIMBUS III the water vapor height profile can be inferred in a cloud-free atmosphere by at least a two parameter method. This offers the possibility to adjust e.g. the total amount and the

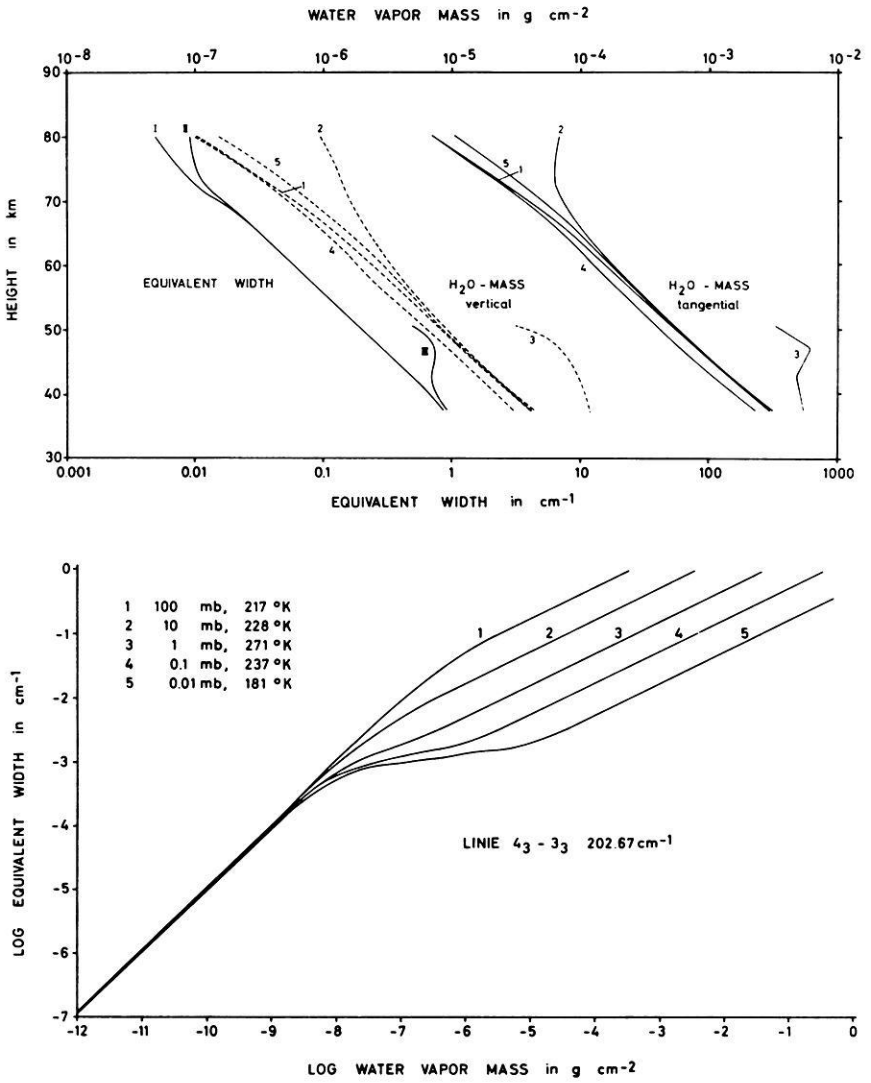

Fig. 15: Upper part: Equivalent width of the line group around 202.67 cm^{-1} in dependence of minimum height above ground (full lines labelled I, II, and III).

The corresponding water vapor mass above of the minimum height (dotted lines) as well as the total water vapor mass in the optical path (full lines) are given for the following cases:

1 Standard atmosphere with mixing ratio 10^{-5} g/g_{air}
2 same as 1, but mixing ratio 10^{-4} g/g_{air} between 82 and 90 km
3 same as 1, but mixing ratio 10^{-4} g/g_{air} between 47.40 and 52.43 km
4 constant temperature 180°K, mixing ratio 10^{-5} g/g_{air}
5 constant temperature 270°K, mixing ratio 10^{-5} g/g_{air}
I, II and III corresponds to the cases 1, 2 and 3.
Lower part: Curves of growth of the central line at 202.67 für different heights.

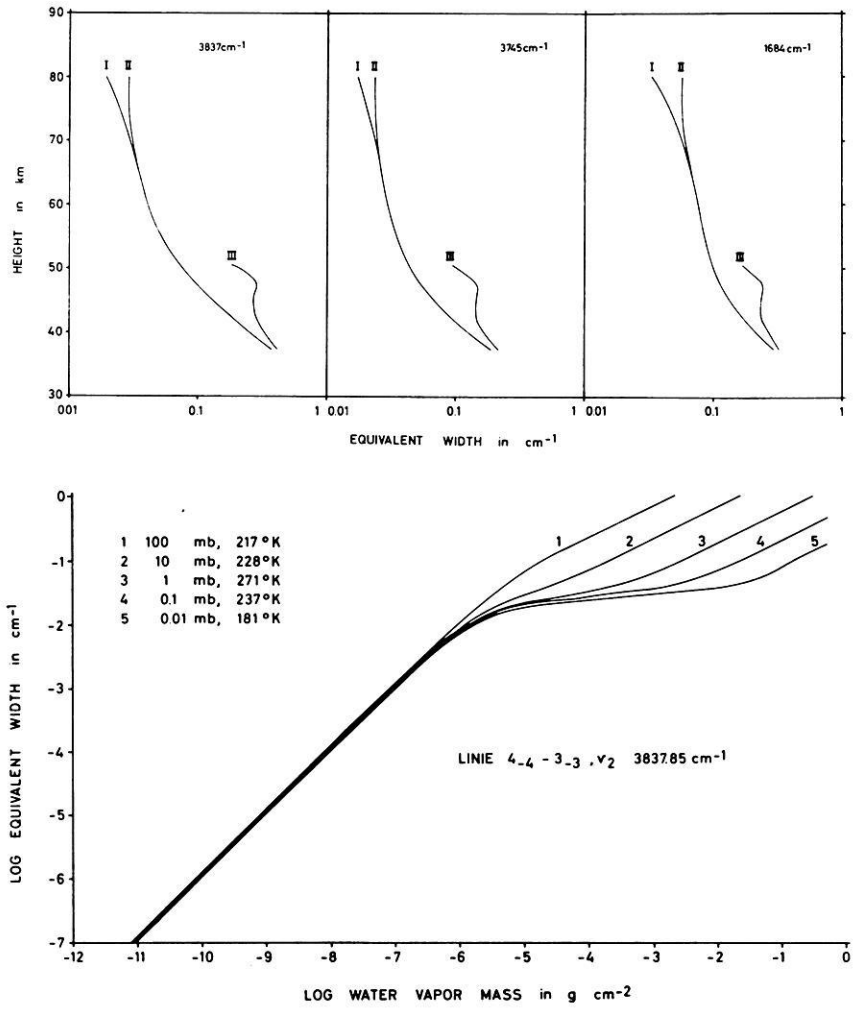

Fig. 16: Upper part: Equivalent widths of line groups at 3837 cm^{-1}, 3745 cm^{-1} and 1684 cm^{-1} for the models 1—3 as in Fig. 15.
Lower part: Curves of growth for a very strong line from these groups as indicated in the figure.

gradient for a given simple type of profile. Broad band radiometric measurements as made from early NIMBUS and TIROS satellites in one water vapor channel with a surface temperature reference give the relative humidity in the upper troposphere under the assumption that this quantity is constant within these levels. From these data the water vapor mass above the 500 mb level can be estimated.

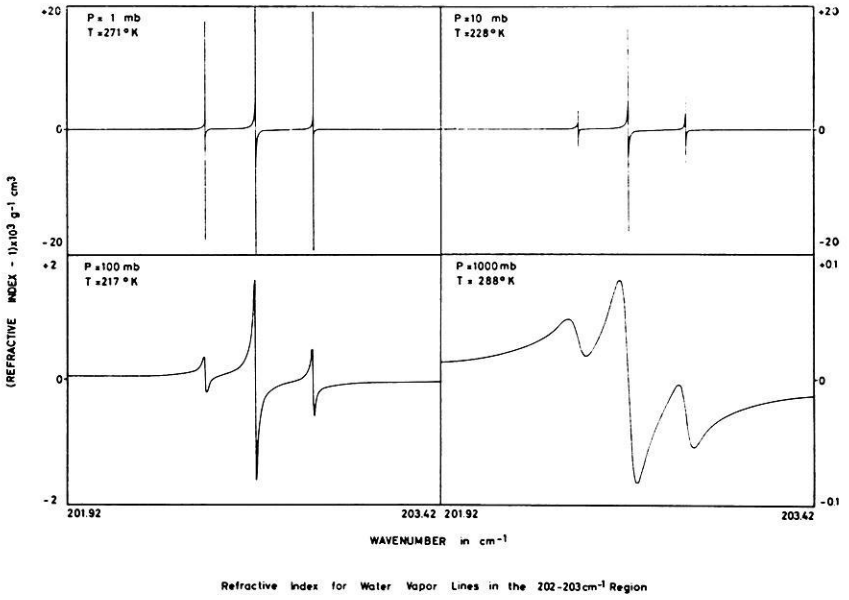

Fig. 17: Index of refraction in different heights for three lines around 202.67 cm^{-1}. The given numbers have to be multiplied with the actual density of the water vapor in g/cm^{-3} in order to be comparable with the standard definition of the index of refraction for air.

Promising for the future is the application of the emission method to multichannel narrow band measurements in the microwave region. Possible wavelength choices are around 1.35 cm or 0.164 cm where water vapor has distinct absorption lines. Most clouds will be transparent for these wavelengths. This technique will therefore also provide water vapor data below clouds. The development of appropriate instrumentation has been initiated in different countries.

Experimental and theoretical work is also in progress to monitor the water vapor at elevated levels above the tropopause at least at sunrise and sunset. However, this experiment requires a satellite with sun stabilization of a quality so far only achieved for the Orbiting Solar Observatory, and an instrument of high spectral resolution.

References

ANDERSON, P. W.: Pressure broadening in the microwave and infra-red regions. Phys. Rev. 76, 647, 1949

BEER, R.: Decrement of the solar continuum in the far infrared. Nature 209, 1226, 1966.

BENEDICT, W. S., and R. F. CALFEE: Line parameters for the 1.9 and 6.3 micron water vapor bands. ESSA Professional Paper No. 2, 1967.

BENEDICT, W. S., and L. D. KAPLAN: Calculation of line widths in H_2O-N_2 collisions. J. Chem. Phys. 30, 388—399, 1959

—: Calculation of line widths in H_2O-H_2O and H_2O-O_2 collisions. J. Quant. Spectr. Radiat. Transfer 4, 543—469, 1964

—: Table of line intensities and half widths of the pure H_2O rotation band. Private communication of Dr. KAPLAN, 1963

BOLLE, H.-J.: Stratospheric water vapor determination by absorption in single lines. Beiträge z. Physik d. Atm. 38, 41—50, 1965

BURCH, D. E., D. A. GRYVNAK, E. B. SINGLETON, W. L. FRANCE and D. WILLIAMS: Infrared absorption by carbon dioxide, water vapor, and minor atmospheric constituents. Opt. Phys. Lab. Proj. 8603 AFCRL-Report 62-698, July 1962

BURCH, D. E., D. A. GRYVNAK and R. R. PATTY: Absorption by H_2O between 2800 and 4500 cm^{-1}. Philco Publ. No. U-3202, Scientific Report, Contract NOnr 3560(00), 30. Sept. 1965

BURCH, D. E., and D. A. GRYVNAK: Absorption by H_2O between 5045—14.485 cm^{-1}. Philco Publication No. U-3704, Scientific Report, Contract NOnr 3560(00), 31. July 1966

CONNES, P.: Principe et réalisation d'un nouveau type de spectrometre interferentiel. Rev. D'Optique 38, 157—201 and 416—441, 1959, and 39, 402—436, 1960

CONRATH, B. J.: On a mathematical formulation of the constituent inversion problem for planetary atmospheres. NASA Report X-622-66-542, October 1966

CONRATH, B. J.: Inverse problems in radiative transfer: A review. NASA Report X-622-67-57, February 1967

—: On the estimation of relative humidity profiles from medium resolution infrared spectra obtained from a satellite. NASA-Report X-622-68-225 Preprint, June 1968

CURTIS, A. R., and R. M. GOODY: Thermal radiation in the upper atmosphere. Proc. Roy. Soc. A., 236, 193—206, 1956

FRITH, R.: Meteorological satellites, future research projects. WMO-Bulletin XI, 202—205, 1962

GATES, D. M., R. F. CALFEE, D. W. HAUSER and W. S. BENEDICT: Line parameters and computed spectra for water vapor bands at 2.7 micron. NBS Monograph 71, 1964

GATES, D. M., D. G. MURCRAY, C. C. SHAW and R. J. HERBOLD: Near infrared solar radiation measurements by balloon to an altitude of 100000 feet. J.O.S.A. 48, 1010—1016, 1958

GOODY, R. M.: Atmospheric radiation, I. Theoretical basis. Clarendon Press, Oxford, 1964

HANEL, R. A., and L. CHANEY: The infrared interferometer spectrometer experiment (IRIS), Vol. II. Meteorological Mission. NASA X-650-65-75, 1965

HERZBERG, G.: Molecular spectra and molecular structure, II. Infrared and raman spectra of polyatmic molecules. D. VAN NOSTRAND Comp., Inc., Princeton, N. J., 1962

HOUGHTON, J. T.: The meteorological significance of remote measurements of infrared emission from carbon dioxide. Quart. J. Roy. Met. Soc. 87, 102—108, 1961

HOWARD, J. N., D. E. BURCH and D. WILLIAMS: Infrared transmission of synthetic atmospheres. III. Absorption by water vapor. J.O.S.A. 46, 242—245, 1956

KING, J. I. F.: Meteorological inferences from satellite radiometry. J. of Atm. Sci., 20, 245 to 250, 1963

KUHN, P. M., and J. D. MCFADDEN: Atmospheric water vapor profiles derived from remote-sensing radiometer measurements. Monthly Weather Review 95, 565—569, 1967

LATKA, R.: Theoretische Untersuchungen zur Gewinnung von Spurengaskonzentrationen aus spektralradiometrischen Messungen. Verh. d. Deutsch. Phys. Ges. 4, 457, 1969

MÖLLER, F.: Atmospheric water vapor measurements at 6—7 microns from a satellite. Planet. Space Sci. 5, 202—206, 1961

—: Einige vorläufige Auswertungen der Strahlungsmessungen von TIROS II. Arch. Met. Geophys. Biokl. Serie B, 12, 78—93, 1962

MURCRAY, D. G., F. H. MURCRAY, W. J. WILLIAMS and F. E. LESLIE: Water vapor distribution above 90,000 feet. J. Geophys. Res. 65, 3641—3469, 1960

NORDBERG, W., A. W. MCCULLOCH, L. L. FOSHEE and W. R. BANDEEN: Preliminary results from NIMBUS II: BAMS 47, 857—872, 1966

OPPENHEIM, U. P., and A. GOLDMAN: Integrated intensity of the 6.3 μ band of water vapor. Appl. Optics 5, 1073—1074, 1966

PALMER, C. H.: Long path water vapor spectra with pressure broadening. I. 20 μ to 31.7 μ, J.O.S.A. 47, 1024—1028, 1957. II. 29 μ to 40 μ, J.O.S.A. 47, 1028—1031, 1957. Experimental transmission functions for the pure rotation band of water vapor, J.O.S.A. 50, 1232—1242, 1960

PICK, D. R., and J. T. HOUGHTON: Balloon-borne measurements of emission in the spectral region 5—8 μ. IAMP/IUGG Symposium on Radiation Including Satellite Techniques. Bergen, Norway, 1968

PRINZ, D. K.: Products of strength times self-broadened half-widths of absorption lines in the ν_2 band of water vapor. Appl. Optics 7, 689—693, 1968

RASCHKE, E.: Auswertung von infraroten Strahlungsmessungen des meteorologischen Satelliten TIROS III. Beitr. z. Phys. d. Atm. 38, 97—120, and 153—187, 1965

RASCHKE, E., and W. R. BANDEEN: A quasi-global-analysis of tropospheric water vapor content and its temporal variations from radiation data of the meteorological satellite TIROS IV. Space Res. VII, North-Holland Publ. Comp., 921—931, 1966

SAKAI, H.: Line strengths and widths in the ν_2 water band. John Hopkins Univ., Final Report CWB 10483, 1964

SMITH, S. D., and C. R. PIDGEON: Application of multiple beam interferometer methods to the study of CO_2 emission at 15 micron. Mem. Soc. R. Sc. Liége, cinquième série, tome IX, 336–349, 1964

SMITH, W. L.: An iterative method for reducing tropospheric temperature and moisture profiles from satellite radiation measurements. Monthly Weather Review, 95, 363–369, 1967

–: Statistical estimation of the atmosphere's pressure-height distribution from satellite radiation measurements. IAMP/IUGG Symposium on Radiation Including Satellite Techniques, Bergen, Norway, 1968

TSAO, C. J., and B. CURNUTTE: Line widths of pressure-broadened spectral lines. J. Quant. Spectr. Rad. Transf. 2, 41–79, 1962

VÖLKER, W.: Ein SISAM-Spektrometer für Okkultationsexperimente an der Atmosphäre. Verh. d. Deutsch. Phys. Ges. 4, 459, 1969

YAMAMOTO, G., and T. ONISHI: Absorption coefficient of water vapor in the far infrared region. Sci. Rep. Tohuku Univ. Series 5, 1, 5–12, 1949, Appendix: 3, 73–77, 1951